High-rate entanglement source via two-photon emission from semiconductor quantum wells

Alex Hayat, Pavel Ginzburg, and Meir Orenstein
Department of Electrical Engineering, Technion, Haifa 32000, Israel
(Received 12 April 2007; revised manuscript received 27 May 2007; published 30 July 2007)

We propose a compact high-intensity room-temperature source of entangled photons based on the efficient second-order process of two-photon spontaneous emission from electrically pumped semiconductor quantum wells in a photonic microcavity. Two-photon emission rate in room-temperature semiconductor devices is determined solely by the carrier density, regardless of the residual one-photon emission. The microcavity selects two-photon emission for a specific signal and idler wavelengths and at a preferred direction without modifying the overall rate. Pair-generation rate in GaAs/AlGaAs quantum well structure is estimated using a 14-band model to be 3 orders of magnitude higher than for traditional broadband parametric down-conversion sources.

DOI: 10.1103/PhysRevB.76.035339 PACS number(s): 42.50.Dv, 03.67.Mn, 32.80.Wr

I. INTRODUCTION

Entangled-photon states are essential in various applications of optical quantum information processing, including quantum computation, quantum cryptography, and teleportation.[1] Furthermore, entanglement highlights most vividly the nonlocality of quantum mechanics through violation of Bell's inequalities,[2] in contrast to the local realism of classical physics.[3]

The earliest attempts to produce polarization-entangled photons by 2-γ photon decay of positronium[4] demanded strong supplementary assumptions for tests of Bell's inequalities due to the lack of high-energy photon polarizers. Pairs of low-energy photons emitted in certain atomic radiative cascades[5] yield better results; however, these sources suffer from low brightness and polarization degradation caused by the atomic recoil. Solid state with higher material density enables a significant increase in the emission rate of the source. The most popular sources of entangled photons today are based on parametric down-conversion (PDC) of pump photons into signal-idler pairs in noncentrosymmetric crystals with second-order optical nonlinearity.[6] The efficiency of PDC-based entanglement sources is limited, however, because of the required postselection or spatial filtering and the relatively weak fundamental interaction. PDC is described by a third-order nonresonant process in the time-dependent perturbation theory[7] combined with a first-order process of the pump laser emission. While the latter process is considerably efficient (typically $\sim$10%), the total probability of the additional 3 orders in the perturbation theory of PDC are proportional to α^3, where α is the fine-structure constant. Moreover, PDC $\chi^{(2)}$ nonlinear interaction requires dispersion compensation techniques using birefringence or quasi-phase-matching.[8] Recently, experiments were performed demonstrating the generation of entangled photons employing standard telecommunication fibers via Kerr nonlinearity,[9] avoiding the output photon fiber-coupling problem and with much less severe phase matching requirements, however, the underlying weaker $\chi^{(3)}$ nonlinearity still limits the source performance. An alternative approach using semiconductor quantum dots (QDs) offers sources of entangled photons on demand;[10] nevertheless, employing QD sources in quantum communications appears to be difficult due to their low generation rates and cryogenic operation.

II. TWO-PHOTON EMISSION BASED ENTANGLEMENT SOURCE

Here, we propose a simple high-efficiency room-temperature entangled-photon source based on spontaneous two-photon emission (TPE) from quantum wells (QWs) in a semiconductor photonic microcavity. The second-order process of TPE is proportional to α^2 and therefore it is expected to be stronger than PDC by at least $10/\alpha$ (about three orders of magnitude) for equal pump levels, while the nonresonant nature of PDC transitions makes this ratio even larger. The QW structure is pumped electrically and a vertical doubly resonant microcavity is designed to preferentially select the two-photon transition wavelength modes: the signal ω_s and the idler ω_i, by methods used for GaAs-based nonlinear optics.[18] Unlike the PDC-based sources,[6] fundamental-wavelength photons (pump) are not required for this process—the energy is stored in the pumped material and one-photon emission may be suppressed. In an ideal TPE-based cavity-controlled source with a forbidden one-photon emission, the majority of the injected carriers will recombine to emit a signal-idler photon pair, which has similar performance as an optically pumped PDC source with conversion efficiency near unity.

Hence, theoretically, such a source should exhibit emission rates higher by many orders of magnitude compared to optically pumped PDC-based sources at the same pump power levels. In practical electrically driven semiconductor devices, however, such high pump powers are not feasible, and at room temperature, the nonradiative recombination will be the dominant process and thus will determine the depletion rate of the carrier density in the QWs. Once the steady-state carrier density in the QWs at a given temperature is determined, the two-photon emission is determined as well, regardless of the residual one-photon emission rate. Therefore, for semiconductor devices operating at room temperature, the two-photon emission rate is determined solely by the carrier density. The photonic microcavity in such devices has a secondary role of reshaping the two-photon spec-

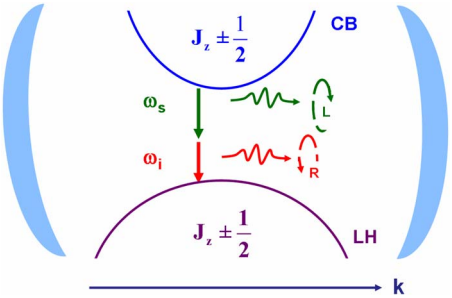

FIG. 1. (Color online) Cavity-controlled two-photon emission entanglement source.

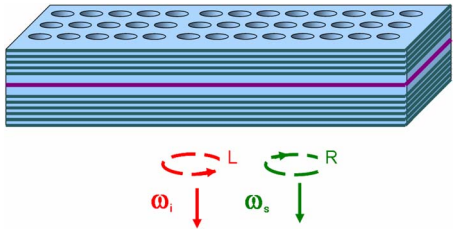

FIG. 2. (Color online) QWs in a vertical cavity combined with 2D photonic crystal, emitting polarization-tagged energy-entangled photons.

trum and emission direction, rather than overall rate enhancement and the suppression of the competing one-photon emission.

In QWs, the light-hole (LH) heavy-hole (HH) degeneracy is removed, decoupling LH and HH levels for electron crystal momentum of $k=0$, and with proper strain, the LH band can have the highest energy, while for nonvanishing k, the LH and HH coupling is finite, dependent on the k value and Luttinger parameters.[11] The vertical double-resonance cavity is designed to constrain the signal and the idler wavelengths to be emitted only by the two-photon transition between the zero-k conduction band (CB) subband edge and the zero-k LH subband edge which are the most populated states under regular injection conditions in such structures. Hence, the angular momentum in the direction of the QW growth, $-z$, in the valence band (VB) is[11] $j_z=\pm 1/2$, and in CB, $j_z=\pm 1/2$. Electron transitions between states of definite angular momentum will result in net angular momentum change of $\Delta j_z=\pm 1$ or $\Delta j_z=0$. The two-photon transitions must have, therefore, total angular momentum change of $\Delta j_z=0$. The cavity with higher reflectivity top mirror will launch the majority of photon pairs to be emitted collinearly downward in the $-z$ direction. Photon pairs emitted collinearly downward will have, therefore, opposite polarizations and can be separated by a polarization beam splitter. The energy conservation for this two-photon process, $\hbar(\omega_i+\omega_s)=E_{CB}-E_{VB}$, does not specify the energy of each individual photon and the emitted two-photon state is, therefore, energy entangled,

$$|\Psi\rangle = \frac{1}{\sqrt{2}}(|\omega_i\rangle_R|\omega_s\rangle_L + |\omega_s\rangle_R|\omega_i\rangle_L), \tag{1}$$

where the entangled particles are identified by the polarization (Fig. 1). At room temperature, the electron angular momentum states will probably be mixed, however, this does not impact the anticorrelated polarizations of the emitted photon pairs for polarization-based separation.

Transitions between angular momentum superposition states in the VB and CB will result in total angular momentum change of $|\Delta j_z|>0$, corresponding to noncollinearly emitted photons with arbitrary polarizations. Only the photons emitted in the z direction can be tagged by polarization and separated by a polarization beam splitter. In order to maximize the vertically propagating emission, a two-dimensional photonic crystal may be added (Fig. 2),[12] similar to the light extraction enhancement techniques used in light emitting diodes. In addition, the Bragg-type vertical cavity itself enhances (reshapes) preferentially the emission along the z direction by increasing the density of photonic states related to this emission. Similar photonic structures based on vertical cavity combined with shallow-corrugation two-dimensional gratings for enhanced-performance light-emitting diodes based on GaAs have been analyzed in detail,[17] yielding extraction efficiencies as high as 40%. Application of such square-lattice grating to TPE emission wavelengths ~ 1.6 μm results in a grating lattice period of ~ 490 nm and filling factor of 0.5, which are feasible using existing fabrication technology.

III. EMISSION RATE CALCULATIONS

Cavity-controlled two-photon emission rate from a QW is calculated by a second-order process in the time-dependent perturbation theory, similar to that of two-photon transition in a single atom.[13] The general expression for the rate is

$$R = \frac{2\pi}{\hbar^2} N_e \int_{\text{radiation states}} F(\omega_1)F(\omega_2)d\omega_1 d\omega_2 \times \sum_{\text{carrier states}} |M|^2 \delta(\omega_0 - \omega_1 - \omega_2), \tag{2}$$

where $\hbar\omega_0$ is the band gap energy, N_e is the number of charge carriers, and $F(\omega)$ is the density of radiation modes. M is given by

$$M = \frac{N_c e^2}{2m_0 c^2}\left(\frac{2\pi\hbar c^2}{V}\right)\frac{1}{\sqrt{\omega_1\omega_2}}M', \tag{3}$$

with electron charge e, free electron mass m_0, and field quantization volume V, determined by the vertical cavity height and the unit cell of the horizontal two-dimensional (2D) photonic crystal. N_c is the number of photonic crystal unit cells for a specific device size and M' is the dimensionless matrix element for the second-order process similar to that of the two-photon absorption:[19]

$$M' = \frac{2}{m_0}\sum_n \left(\frac{\langle f|\hat{p}\vec{\varepsilon}_2 e^{-ik_2 x}|n\rangle\langle n|\hat{p}\vec{\varepsilon}_1 e^{-ik_1 x}|i\rangle}{E_i - E_n - \hbar\omega_1} + \frac{\langle f|\hat{p}\vec{\varepsilon}_2 e^{-ik_2 x}|n\rangle\langle n|\hat{p}\vec{\varepsilon}_1 e^{-ik_1 x}|i\rangle}{E_i - E_n - \hbar\omega_2} \right), \quad (4)$$

where $\hat{p}$ is the momentum operator, $\vec{\varepsilon}$ is the photon polarization, and i, n, and f are the initial, intermediate, and final electron states, respectively.

Considering the initial state as the ground subband of the QW in the CB and the final state as the ground subband of the QW in the LH band, we base our calculations on a 14-band model[14] taking into consideration only the $p(\Gamma_7)$, $p(\Gamma_8)$, $p(\Gamma_8)$, $\tilde{s}(\Gamma_6)$, $\tilde{p}(\Gamma_7)$, $\tilde{p}(\Gamma_8)$, and $\tilde{p}(\Gamma_8)$ with two spin states, with the higher conduction bands $\tilde{p}(\Gamma_7)$ and $\tilde{p}(\Gamma_8)$ taken as the intermediate states, while the other bands are neglected due to their energy remoteness.

Transitions between electrons states with high lattice momentum have larger matrix elements due to their k dependence;[11] however, they are less populated by carriers. Nevertheless, the deterioration of the photon polarization anticorrelation due to these transitions can be minimized by the proposed vertical wavelength-selective cavity designed to match the $k=0$ transition.

The dipole matrix elements for the $p(\Gamma_7)$, $p(\Gamma_8)$, and $\tilde{s}(\Gamma_6)$ intermediate states are k dependent, and being suppressed by the zero-k selecting cavity, will not contribute to the overall emission rate. Therefore, the two-photon transition probability can be calculated by using only the higher conduction bands $\tilde{p}(\Gamma_7)$ and $\tilde{p}(\Gamma_8)$ as intermediate states. Due to selection rules, the envelope functions have equal quantum numbers, and the calculation of the matrix elements between the following states is performed using the dipole approximation:

$$\left|\frac{1}{2},\frac{1}{2}\right\rangle_{electrons} = |i\rangle = |S_\uparrow\rangle \cdot \phi_e(z) \cdot e^{j\vec{k}_e\cdot\vec{\rho}},$$

$$\left|\frac{3}{2},\frac{1}{2}\right\rangle_{light\text{-}hole} = |f\rangle = \left[\sqrt{\frac{2}{3}}|Z^v_\uparrow\rangle - \sqrt{\frac{1}{6}}|(X^v + iY^v)_\downarrow\rangle\right]\phi_{lh}(z)\cdot e^{j\vec{k}_{lh}\cdot\vec{\rho}},$$

$$|n_1\rangle = \sqrt{\frac{1}{2}}|X^c_\uparrow + iY^c_\uparrow\rangle \cdot \phi_{pe}(z)\cdot e^{j\vec{k}_{pe}\cdot\vec{\rho}},$$

$$|n_2\rangle = \left[\sqrt{\frac{1}{3}}|Z^c_\downarrow\rangle - \sqrt{\frac{1}{3}}|X^c_\uparrow - iY^c_\uparrow\rangle\right]\cdot\phi_{pe}(z)\cdot e^{j\vec{k}_{pe}\cdot\vec{\rho}}, \quad (5)$$

where ϕ_i are the envelope functions, k is the in-plane electron crystal momentum, $\uparrow$ and $\downarrow$ represent the spin state, and X, Y, and Z are the periodic parts of Bloch functions. The other pair of final and initial states ($|f\rangle = |3/2,-1/2\rangle$ and $|i\rangle = |1/2,-1/2\rangle$) leads to the same rate and the same allowed photon polarizations. For the chosen intermediate states, the infinite summation in Eq. (4) is replaced by only two nonvanishing different terms. Calculation of two-photon emission for x-polarized photons can be applied to the y-polarized emission as well, due to the z-axis rotation symmetry, and thus both right and left polarized photon transitions will have equal probabilities. The overlap of the different-band same-quantum-number envelope functions in infinite-barrier QW is unity, which is a good approximation for the QW structure used in our calculations. Using the noncentrosymmetric zinc blende 14-band model matrix elements[14] yields

$$M' = i\sqrt{\frac{3}{2}}\frac{P_1 Q}{m_e}\left(\frac{1}{E_c+\hbar\omega_s} + \frac{1}{E_c+\hbar\omega_i} - \frac{1}{E_c+\hbar\omega_s-\Delta_c} - \frac{1}{E_c+\hbar\omega_i-\Delta_c}\right), \quad (6)$$

where P_1 and Q are the dipole moments for specific transitions, E_c is the s-p band energy difference, and Δ_c is the higher conduction band energy splitting.

For the in-plane-propagating z-polarized two-photon emission, the matrix element is four times larger than that of the vertical propagation; however, it is suppressed by the proposed photonic crystal. The two-photon transition with different, i.e., in-plane and vertical, polarizations is totally forbidden. Assuming the cavity-controlled density of states $F(\omega)$ to consist of two well-separated Lorentzians:

$$F(\omega) = \frac{1}{2\pi}\left\{\frac{\omega_s/(2Q_s)}{(\omega-\omega_s)^2 + [\omega_s/(2Q_s)]^2} + \frac{\omega_i/(2Q_i)}{(\omega-\omega_i)^2 + [\omega_i/(2Q_i)]^2}\right\}. \quad (7)$$

The calculated vertical emission rate is

$$R = \frac{\pi^3 e^4 N_c}{m_0^2 V} n_e \frac{|M'|^2}{\omega_0\omega_i\omega_s}, \quad (8)$$

where $n_e = N_e/V$ is the charge carrier density.

Usually, in the one-photon Purcell effect,[15] the overall narrow-band one-photon emission, and hence the electron decay rate, is increased by modifying the cavity photon density of states to match the narrow-band free-space emission spectrum. In two-photon emission, however, the free-space emission spectrum is very wide band, due to the different combinations of signal and idler wavelengths. For wide-band emitters placed in narrow-band cavities, the photon density of states has no effect on the overall emission intensity.[16] Therefore, the cavity only determines the emitted spectrum shape and the angular distribution of the emission but does not increase the overall electron decay rate. This is demonstrated by our calculated cavity-controlled two-photon emission rate, which does not depend on the cavity's quality factor [Eq. (8)].

IV. RESULTS

Assuming that only the vertical emission is allowed by the photonic crystal, we calculate the pair-generation rate for a structure of GaAs/AlGaAs QWs, injected carrier density of $n_e \sim 10^{19}$ cm^{-3}, and a 1 mm^2 device surface area. Vertical cavity is designed to support both signal and idler wave-

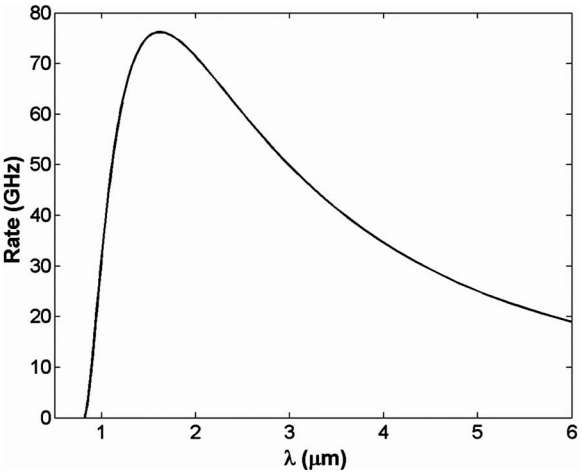

FIG. 3. Entangled pair-generation rate vs one of the two-photon emission wavelengths.

lengths and its physical dimensions are chosen to be approximately half of the harmonic average of emitted-photon wavelengths, whereas further enlargement of the vertical cavity height would decrease the two-photon emission rate [Eq. (8)].

In order to take into consideration the impact of many-body effects[23] on the emission rate, we calculated rate modification due to carrier-carrier scattering, band gap renormalization, and Coulomb enhancement.[20–23] These phenomena were shown to have a significant impact on overall free-space emission;[22] however, for the zero-k transition dictated by the cavity, the rate change is calculated to be less than 2%.

The maximal entangled pair-generation rate for a half-wavelength vertical cavity size is $R \sim 7.5 \times 10^{10}$ s^{-1} (Fig. 3). This rate corresponds to $\tau_{2ph} \sim 13$ ps average time interval between two-photon emission processes, and for a quality factor Q of 1000, the cavity photon lifetime is $\tau_{cav} \sim 2.4$ ps. Very high TPE rates combined with $Q \sim 1000$ may cause mixing between photon pairs from different two-photon transitions. However, for the calculated rate and Q, no more than one-photon pair exists in the cavity at any given moment, preventing the deterioration of entanglement. The theoretically demonstrated narrow bandwidth room-temperature device rate is 3 orders of magnitude higher than that of the traditional broadband PDC-based sources.[8] At lower temperatures with reduced nonradiative recombination rate, much higher emission rates are achievable.

V. CONCLUSIONS

In conclusion, we have demonstrated that a compact highly efficient entangled-photons source can be realized via microcavity-controlled two-photon spontaneous emission from semiconductor QWs at room temperature. The microcavity is not expected to increase the total two-photon decay rate; nonetheless, the desired wavelength emission is enhanced while the rest of the spectrum is suppressed. The significantly more efficient second-order fundamental interaction, narrow bandwidth, and collinear photon emission strongly enhance the efficiency, leading to tens of gigahertz pair-generation rates, which are 3 orders of magnitude higher than those of the broadband PDC-based sources. Furthermore, small dimensions, integrability, narrow bandwidth, and room-temperature operation of this source may help introduce quantum information processing such as teleportation, quantum cryptography, and quantum repeaters into the existing infrastructure of fiber-optical communications and integrated photonics.

[1] C. H. Bennett and S. J. Wiesner, Phys. Rev. Lett. **69**, 2881 (1992).
[2] J. F. Clauser, M. A. Horne, A. Shimony, and R. A. Holt, Phys. Rev. Lett. **23**, 880 (1969).
[3] A. Einstein, B. Podolsky, and N. Rosen, Phys. Rev. **47**, 777 (1935).
[4] A. R. Wilson, J. Lowe, and D. K. Butt, J. Phys. G **2**, 613 (1976).
[5] A. Aspect, P. Grangier, and G. Roger, Phys. Rev. Lett. **47**, 460 (1981).
[6] P. G. Kwiat, K. Mattle, H. Weinfurter, A. Zeilinger, A. V. Sergienko, and Y. Shih, Phys. Rev. Lett. **75**, 4337 (1995).
[7] R. Boyd, *Nonlinear Optics*, 2nd ed. (Academic, New York, 2003).
[8] M. Pelton, P. Marsden, D. Ljunggren, M. Tengner, A. Karlsson, A. Fragemann, C. Canalias, and F. Laurell, Opt. Express **12**, 3573 (2004).
[9] X. Li, P. L. Voss, J. E. Sharping, and P. Kumar, Phys. Rev. Lett. **94**, 053601 (2005).
[10] N. Akopian, N. H. Lindner, E. Poem, Y. Berlatzky, J. Avron, D. Gershoni, B. D. Gerardot, and P. M. Petroff, Phys. Rev. Lett. **96**, 130501 (2006).
[11] G. Bastard, *Wave Mechanics Applied to Semiconductor Heterostructures* (Les Editions de Physique, Les Ulis, 1988).
[12] K. Sakoda, *Optical Properties of Photonic Crystals* (Springer, Berlin, 2005).
[13] L. S. He and X. L. Feng, Phys. Rev. A **49**, 4009 (1994).
[14] M. E. Flatté, P. M. Young, L.-H. Peng, and H. Ehrenreich, Phys. Rev. B **53**, 1963 (1996).
[15] C. Santori, D. Fattal, J. Vuckovic, G. S. Solomon, and Y. Yamamoto, Nature (London) **419**, 594 (2002).
[16] R. Coccioli, M. Boroditsky, K. W. Kim, Y. Ramhat-Samii, and E. Yablonovitch, Proc. Inst. Electr. Eng. **145**, 391 (1998).
[17] D. Delbeke, P. Bienstman, R. Bockstaele, and R. Baets, J. Opt. Soc. Am. B **19**, 871 (2002).
[18] G. Klemens, C.-H. Chen, and Y. Fainman, Opt. Express **13**, 9388 (2005).
[19] C. C. Lee and H. Y. Fan, Phys. Rev. B **9**, 3502 (1974).
[20] C. F. Hsu, P. S. Zory, Jr., C.-H. Wu, and M. A. Emanuel, IEEE J. Sel. Top. Quantum Electron. **3**, 158 (1997).
[21] W. W. Chow and S. W. Koch, *Semiconductor-Laser Fundamentals* (Springer, Berlin, 1999).
[22] M. Kira and S. W. Koch, Prog. Quantum Electron. **30**, 155 (2006).
[23] H. Haug and S. W. Koch, Phys. Rev. A **39**, 1887 (1989).